

INVESTIGATION OF LOCAL OPENING-SLIDING RELATIONSHIP IN THE VICINITY OF DEFORMED BAR IN CONCRETE BY USING DIC TECHNIQUE

A. OKEIL^{*}, R. UPADHYAY[†], K. MATSUMOTO^{††} AND K. NAGAI^{†††}

^{*} The University of Tokyo
Tokyo, Japan
E-mail: okeil@iis.u-tokyo.ac.jp

[†] Delhi Technological University
Delhi, India
E-mail: rheupadhyay04@gmail.com

^{††} The University of Tokyo
Tokyo, Japan
E-mail: km312@iis.u-tokyo.ac.jp

^{†††} The University of Tokyo
Tokyo, Japan
E-mail: nagai325@iis.u-tokyo.ac.jp

Key words: Local bond, Crack propagation, Aggregates, Deformed bars, Image processing

Abstract: One of the important factors affecting the behaviour of a reinforced concrete (RC) is the bond between concrete and the reinforcement bars. To model the bond between concrete and the reinforcement in the numerical simulation of a RC, accurately modelling for the reinforcing bar with its ribs in 3D shape is required. So to simulate the bond behaviour between concrete and steel rebar, the contact surface between them is represented by normal and shear behaviours. The characteristics of these springs are modified based on numerical simulations to get best-matched results to the experimental results. Therefore, in this study, the opening-sliding relationships between a deformed bar and surrounding matrix are investigated experimentally by using digital images correlation (DIC) technique. A standard axial tension test was applied to a deformed steel bar that was embedded in concrete and cement paste specimen. The specimen had a trapezoidal “window,” which allows full continuous observation and measurements of concrete or cement paste displacements by recording high-resolution digital video that was later analysed by DIC software. The half of the steel bar’s cross-section was removed to see directly the ribs of the rebar and thereby capture the local deformations between these ribs. For that purpose 15 points were chosen, at the tips of the ribs and also between the ribs of the deformed bar, to investigate the relative displacements between the deformed bar and surrounding matrix in X-direction and Y-direction. Based on the results of the experiments, some relationships between opening and sliding in case of cement paste or concrete were established. It was found that the opening between the concrete and the rebar at the tip of the rib is higher than between the ribs. Also, the sliding between the concrete and the rebar at the tip of the rib is higher than between the ribs.

1 INTRODUCTION

Concrete-steel composite is widely used as a structural material. The bond between concrete and steel is necessary not only to ensure adequate level of safety allowing composite action of steel and concrete, but also to control structural behavior along with sufficient ductility. Bond can be achieved between steel bars and concrete in an RC member the mechanical action of ribs of the deformed bar and surrounding concrete. Several experimental studies have been completed to investigate average local and macro response of the bond, and according to these studies several bond models have been successfully reported [1, 2, 3]. Different parameters such as concrete cover, concrete strength, casting direction, elasticity and shape of the rebar were studied while investigating bond behavior [1, 4].

Several experimental studies have been showed the influence of deformation patterns and rib geometry on bond [5, 6, 7]. Local cracks which are formed around deformed bar inside the concrete, affect the bond and those local cracks were successfully observed and schematic diagram represents these cracks was established by (Y. Goto, 1971) [7]. Studies have shown that the aggregate surface area has a significant influence on the mechanical properties of mortar and thereby the bond between deformed bars and surrounding concrete [8].

Based on these global observations, there was a need to simulate bond behavior to predict the performance of the reinforced concrete structures in the future. Meanwhile, computer performance has dramatically improved so that the simulation by modelling the shape of the deformed steel bars becomes possible. It was found that to simulate macroscopic bond behavior; it is necessary to introduce interfacial transition zone around the deformed bar [9]. This porous zone is characterized by reduced tensile strength and elastic modulus of concrete by half due to wall effect [9, 10].

Recently, using digital image correlation

(hereafter referred to DIC) technique to analyze material properties such as concrete has become easier [11, 12, 13]. Study of the bond at the local level with direct observation and measurements of the displacements near the ribs of the deformed bar and thereby strains were recently introduced by using DIC software. Few studies on this technique have shown the applicability of using such a technique in standard pull-out tests in which one deformed bar is embedded centrally in concrete specimen [14].

Regarding this substance, it is very important to investigate the bond behavior in RC experimentally by using advanced techniques, which will enhance our understanding regarding all bond cases and help to improve current bond models in the future. In this study, a powerful experimental procedure for monitoring, and examining of such local deformations between ribs of steel rebar and concrete or cement paste has been proposed, which helps in better understanding of local bond behavior between rebar and concrete, and the mechanisms which govern this behavior. This study also aims to investigate the deformational state under keeping the loading, resulting in that it enables to capture the deformations under the corresponding load levels quantitatively.

2 EXPERIMENTAL PROGRAM

2.1 Materials

Two types of specimens were used in this study; one with concrete and the other with cement paste. Ordinary Portland Cement (OPC) was used as the main binder for both. The water-to-cement ratio (w/c) was 60% by weight. The maximum size of aggregate was 20 mm as generally used in construction projects in Japan. Three standard cylinders of size (100 mm x 200 mm) were used to determine the compressive strength of the concrete and cement paste. Details of the concrete and cement paste mixtures and their strengths are given in Table 1.

Table 1: Mix proportions and fresh properties of concrete and cement paste

	Concrete	Cement Paste
Water (kg/m ³)	180	654
Cement (kg/m ³)	300	1090
Sand (kg/m ³)	807	-
Gravel (kg/m ³)	1008	-
Slump (mm)	90	-
Compressive Strength (MPa)	28.5	24

Table 2: Material properties of reinforcing bar

Diameter (mm)	Yield strength (MPa)	Modulus of Elasticity (MPa)
25	490	190,000

Screw deformed steel bars 25 mm in diameter and 2200 mm long were used for all specimens. Half of the steel bar cross-section was removed to allow directly observation of the rebar ribs and to investigate local deformations between the ribs. This was thought useful for clarifying and understanding behavior in this zone. A metal laser cutting machine was used to remove half of the cross-section (as shown in Figure 1). The properties of the reinforcement are listed in Table 2.

2.2 Test specimen

The set-up of this experiment was performed according to a standard axial tension test and it is shown in Figure 2. Two types of specimens were examined: concrete specimens and cement paste specimens. The test specimen was basically a rectangular of 150 mm x 150 mm x 150 mm. A single screw-shaped reinforcing bar (rebar) was cast in the center of the cross-section. The length of the specimen was determined to be limited as much as possible so that specimen could be easily handled, but at the same time long enough to include a ‘window’ without affecting the stress distribution. For direct monitoring and observation purpose of the interface between the rebar and the concrete or cement paste, the specimen formwork was not completely casted with concrete or cement

paste. Instead, a trapezoidal void was formed during casting by using a ‘foam’ material (refer to Figure 3). This ‘window’ might affect the stress distribution inside the specimen due to breaking the symmetry of the specimen. On the other hand, it has an advantage which is allowing close and continuous monitoring and observation of the displacements in the concrete and cement paste. It was found that the height of the ‘window’ should equal to one-fifth of the total height of the specimen to minimize as much as possible the stress disturbance while at the same time allowing appropriate lightening of the area targeted [9].

2.3 Mixing, casting and curing

The bars were placed horizontally and in the center of the formworks. Concrete or cement paste was poured vertically. Lubricating oil was applied on all sides of the molds for easy removal of specimens. Concrete was poured carefully from the top and segregation was avoided. Needle vibrator was used to compact the concrete. After twenty four hours the specimens were demolded and cured by being covered with wet cloth from just after removing the form to the day before the test in order to avoid the drying shrinkage.

2.4 Technical requirements

Digital image correlation (DIC) system was used to obtain local deformations such as displacements from high-resolution video recorded during experiments (GOM Correlate [15]). Prior to run the DIC analysis, images had to be extracted from the video with same parameters; the software FFmpeg was used for that process [16].

GOM correlate can clearly identify areas of a measurement image which contains sufficient image information for analysis, and then identify the same areas in other images. These areas called “square facets,” and the software recognizes them by their stochastic pattern structure, and the facets must have a unique gray level distribution which can be clearly identified. The term stochastic pattern means that it is a pattern that is as random as

possible. This can be achieved by spraying the surface of the concrete or cement paste with a thin layer of white paint then black dots as shown in Figure 4.

High-resolution video camera (4k) was used for recording during the test. The resolution of the camera (i.e., the number of pixels per area in an image) is 3840 pixels \times 2160 pixels, to catch very local deformations. The distance between the lens and the surface of the specimen was 10 cm.

2.5 Test procedure

The testing apparatus for axial tension loading is shown in Figure 5. The tensile force was applied to the specimen which was set horizontally on the floor. One end of the deformed bar protruding from the end of the specimen was fixed to the steel frame, which was designed especially for this test, and the tensile force was applied to another end of the bar. The thickness of the steel frame was designed to make the specimen floating and not touching the floor when it is fixed with the steel frame.

As shown in Figure 2, three contact-type displacement transducers (LVDT) were used at different positions (1, 2 and 3) to determine the relative displacement between the deformed bar and the specimen. Actual relative displacement (R.D) between the matrix and the rebar was calculated according to Eq. 1.

$$R.D = \delta 1 - \delta 2 - \delta 3 \quad (1)$$

Where, δ represents the values measured by the LVDTs.

For all tests, the loading rate was kept to about 1 kN/5s by adjusting the speed of the hydraulic pump, and the images were extracted from the video as one image every five seconds to match loading rate.

3 RESULTS AND DISCUSSIONS

Figure 6 shows the load relative displacement response of concrete and cement paste specimens with half cross-section deformed bars. Loading was interrupted twice during the test to verify correct functioning of

the system and to check the status of cracks inside the window. The maximum load (Fmax) was about 125 kN because of the reduced cross-section of the deformed bar, which reduced the yield point of the steel to almost half its value which was supposed to be 250 kN.

After finishing the loading process and while monitoring and analyzing the video for the concrete specimen, it was noticed that at the vicinity of the deformed bar, the concrete parts had an intention to move in the direction perpendicular to the rebar which causing opening also between concrete and rebar, not only sliding. So it is important to investigate the opening-sliding relationship between the deformed bar and surrounding matrix. For that purpose, 15 points were chosen, at the tips of the ribs and also between the ribs, to investigate the relative displacements between the deformed bar and surrounding matrix in X-direction and Y-direction (as shown in Figure 7).

3.1 Investigating horizontally along the deformed bar

Figure 8 shows the opening-sliding relationships between concrete and steel bar for 15 points. These points were chosen at distance (1 mm – 1.5 mm) from the surface of the deformed bar. The relationships are divided into four graphs (a, b, c and d). Graph (a) present the points at the tips of the ribs to the left of the central line of loading, graph (b) those at the tips of the ribs to the right of the central line of loading, graph (c) those between the ribs to the left of the central line of loading and graph (d) those between the ribs to the right of the central line of loading.

It is clear that the opening between the concrete and rebar at the tip of the rib (graph (a) and (b)) is higher than those between the ribs (graph (c) and (d)). Also, it is clear that the sliding between the concrete and the rebar at the tips of the ribs (graph (a) and (b)) is higher than those among the ribs (graph (c) and (d)). Here, the main cracks developed and appeared outside the window to the left side of point 1 and to the right side of the point 15. So

it can be noticed that at the same sliding, the opening at points which are far from the main crack is higher than that near the main crack. Also, at points far from the main crack, the opening is much higher than the sliding comparing to points near the main crack. In addition, it can be concluded that, far from the main crack, the inclination or the slope of the opening-to-sliding ratio changes by (2:1), meanwhile, near the main crack it shifts from (2:1) to (1:3).

Figure 9 shows also the opening-sliding relationships for 15 similar points but for the cement paste specimen. The categorization is same as for the concrete case (a, b, c and d). In cement paste case, the trend is much easier to catch than the concrete. It is very clear that the relation between the opening and the sliding is roughly linear; and the slope of their ratio changes from 3:1 far from the main crack to 1:1 near the main crack. It can be seen that the opening between the cement paste and the rebar at the tip of a rib is higher than between the ribs. Also, at the same sliding, the opening at points which are far from the main crack is higher than that near the main crack. Therefore, the difference between the concrete and the cement paste; in case of cement paste, the difference between points is somehow constant because the softening of cement paste is very low comparing to the concrete. As a result, few cracks can be found in cement paste rather than concrete but these cracks are very much wider than those in concrete. So the opening and sliding of the cement paste depends on the displacement of the crack, because it is a homogenous material. Meanwhile, in the case of concrete, opening and sliding depends on the number of cracks and the stiffness of the coarse aggregate particles as it is non-homogenous material.

3.2 Investigating vertically along the deformed bar

To investigate deeply the surrounding zone around the deformed bar, two points were chosen to be more investigated for the same opening-to-sliding relationship. These points were chosen to be far as much as possible

from the main cracks to not be affected by the characteristics of these cracks. These two points were investigated for the relative displacements in X and Y directions between the rebar (fixed point) and the surrounding concrete or cement paste at 1 mm, 3 mm, 5 mm, 7 mm and 9 mm from the face of the rebar (refer to Figure 10). For the concrete case, points 3 and 4 were chosen for the investigation and for the cement paste case, points 2 and 3 were chosen. Figure 11 shows two graphs for the opening-sliding relationships of points 3 and 4 in the concrete case, while Figure 12 shows the same relationships but for points 2 and 3 in the cement paste case. From Figure 11, it is clear that both points 3 and 4 at all locations inside the concrete are moving almost like a rigid body till 70% of F_{max} (at 0.25 mm sliding), while after 70% of F_{max} , the trend of the each point at 1 mm is totally different from other locations. This deformational behavior could be explained by the shear interface zone deterioration which is concentrated around 1-2 mm from the face of the rebar.

It is also clear from both graphs of the concrete (as shown in Figure 11), as going far from the surface of the rebar, the opening between concrete and the rebar increases more than sliding, which means that with going far vertically from the rebar, the opening becomes more dominant. This could be explained by Figure 12, as the internal stress inside concrete progresses, there are numerous micro cracks which occur between these locations (1 mm - 3 mm - 5 mm - 7 mm - 9 mm) due to the heterogeneity of the concrete material, so the opening between the rebar and concrete at location of 5 mm will be a cumulative opening from 0 mm till 5 mm.

4 CONCLUSIONS

This paper presents an experimental study of axial tension tests of deformed bars in concrete and cement paste specimens. For direct monitoring and observation purpose of the interface between the rebar and the concrete or cement paste, each specimen have

a trapezoidal which was formed during casting. DIC analysis was used to visualize local behavior within the concrete or cement paste. The following conclusions have been drawn from this work:

1. The DIC technique was used to find the normal stresses at the interface between concrete and steel that result in opening between concrete or cement paste and rebar.
2. The opening between concrete and rebar at the tip of a rib is greater than between ribs. Also, it was found that sliding between concrete and rebar at the tip of a rib is higher than between ribs. For a certain amount of sliding, the opening at points far from the main crack is greater than at those near the main crack. At points far from the main crack, the opening is much higher compared to the sliding, in contrast with points near the main crack.
3. In the case of cement paste, the relation between opening and sliding is roughly linear and stable. Moreover, the opening between cement paste and rebar at the tip of a rib is higher than between the ribs.
4. As going far from the surface of the rebar, the opening between concrete and the rebar increases more than sliding, which means that with going far vertically from the rebar, the opening becomes more dominant.

REFERENCES

- [1] H. Shima, L. L. Chou, and H. Okamura, "Micro and macro models for bond in reinforced concrete," *Journal of the Faculty of Engineering*, 39(2), 133-194, 1987.
- [2] R. Eligehausen, E. P. Popov, and V. V. Bertero, "Local bond stress-slip relationships of deformed bars under generalized excitations," University of California, Report no. UCB/EERC-83/23 of the National Science Foundation, 1983.
- [3] L.A. Lutz and P. Gergely, "Mechanics of bond and slip of deformed bars in concrete," *ACI Journal*, 64(11), 711-721, 1967.
- [4] B. S. Hamad, "Bond strength improvement of reinforcing bars with specially designed rib geometries," *ACI structural journal*, 92(1), 3-13, 1995.
- [5] B. B. Broms, "Technique for investigation of internal cracks in reinforced concrete members," *ACI Journal, Proceedings*, 62(1), 35-44, 1965.
- [6] D. Watstein, and R. G. Mathey, "Width of Cracks in Concrete at the Surface of Reinforcing Steel Evaluated by Means of Tensile Bond Specimens," *ACI Journal*, 56(1), 47-56, 1959.
- [7] Y. Goto, "Cracks formed in concrete around deformed tension bars," *ACI Journal*, 68(4), 244-251, 1971.
- [8] C. F. Goble, and M. D. Cohen, "Influence of aggregate surface area on mechanical properties of mortar," *ACI materials Journal*, 96(6), 657-662, 1999.
- [9] H.M. Salem, and K. Maekawa, "Pre-and post-yield finite element method simulation of bond of ribbed reinforcing bars," *Journal of Structural Engineering*, 130(4), 671-680, 2004.
- [10] L. Eddy, K. Matsumoto, K. Nagai, and Z. Wang, "Investigation of effect of local bond model on crack propagation in RC using 3D RBSM," *Proceedings of Euro-C 2018, Bad Hofgastein, Austria, 26 February - 1 March 2018*.
- [11] D. Corr, M. Accardi, L. Graham-Brady, and S. Shah, "Digital image correlation analysis of interfacial de-bonding properties and fracture behavior in concrete," *Engineering Fracture Mechanics*, 74(1), 109-121, 2007.
- [12] J. Kozicki, and J. Tejchman, "Experimental investigations of strain localization in concrete using Digital Image Correlation (DIC) technique," *Archives of Hydro-Engineering and Environmental Mechanics*, 54(1), 3-24, 2007.
- [13] S.G. Shah, and J.M Chandra Kishen, "Determination of fracture parameters of concrete interfaces using DIC," *Fracture Mechanics of Concrete and Concrete*

Structures, 1208-1215, 2010.

- [14] O. Leibovich, A. N. Dancygier, and D. Z. Yankelevsky, “An Innovative Experimental Procedure to Study Local Rebar-Concrete Bond by Direct Observations and Measurements,” *Experimental Mechanics*, 56(5), 673-682, 2016.
- [15] GOM Correlate (2016), “Inspection and Testing Guide,” available at <http://www.gom.com/index.html>. Accessed Aug. 2014.
- [16] F. Bellard, M. Niedermayer, FFmpeg, <http://ffmpeg.org>, 2012



Figure 1: Cutting half of the cross section of the rebar by laser cutting

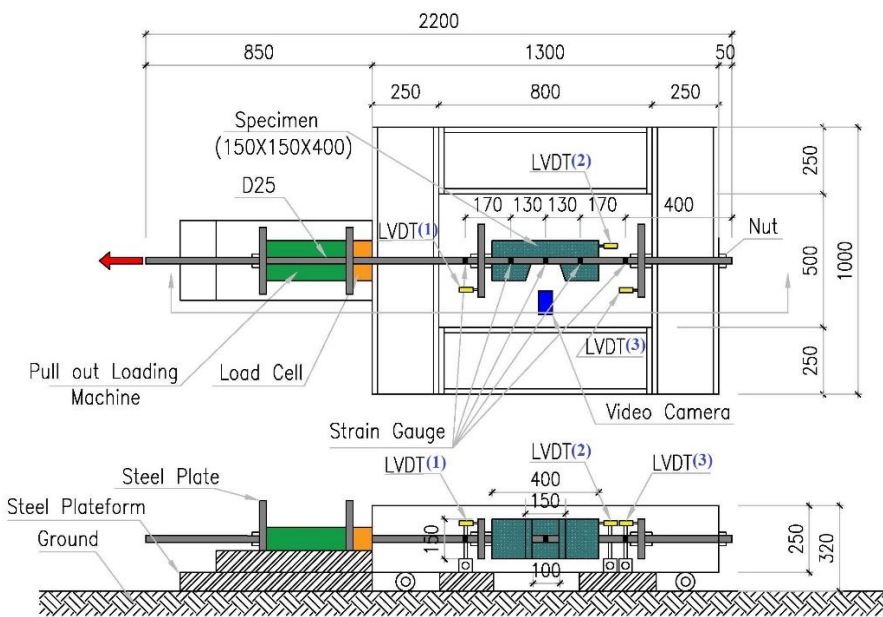


Figure 2: The set-up of the experiment

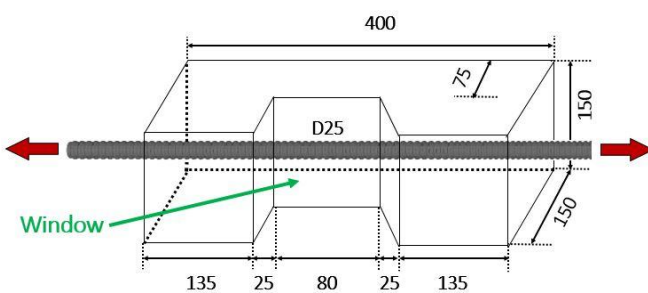


Figure 3: Lay-out of the test specimen (units: mm)

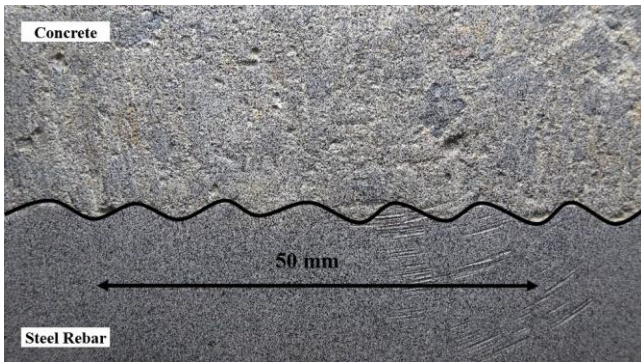


Figure 4: Sprayed specimen of the photographed area of interest



Figure 5: Testing apparatus and steel frame of the test

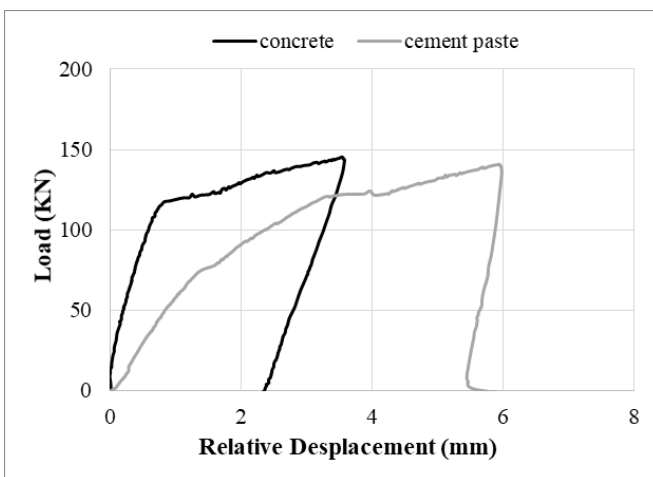
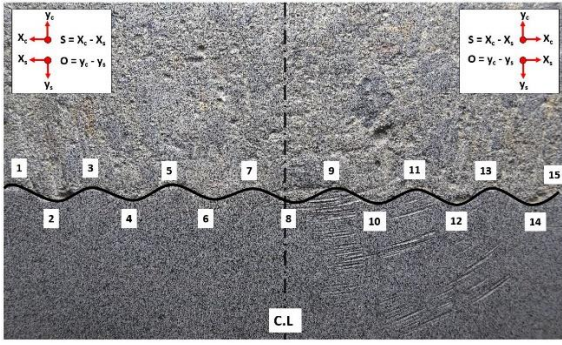
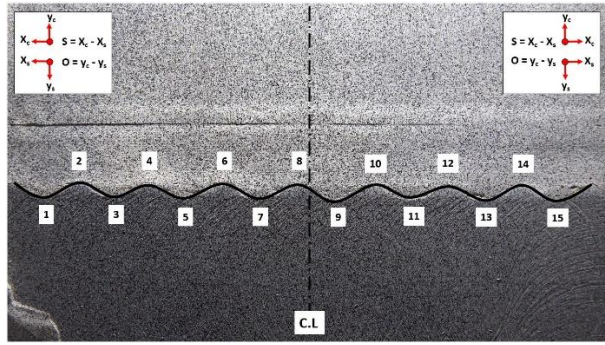


Figure 6: Load-relative displacement relationships

Concrete

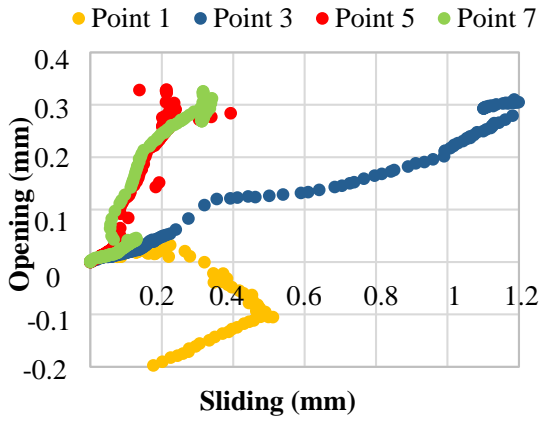


Cement Paste

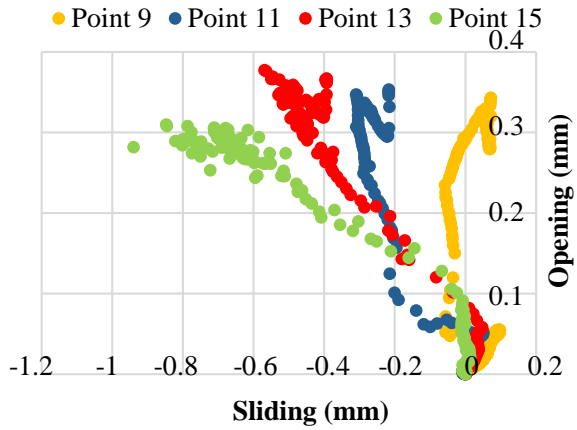


Note: S is sliding between matrix and rebar, O is opening between matrix and rebar, X_c, Y_c are displacements of matrix in X, Y directions respectively, X_s, Y_s are displacements of rebar in X, Y directions respectively

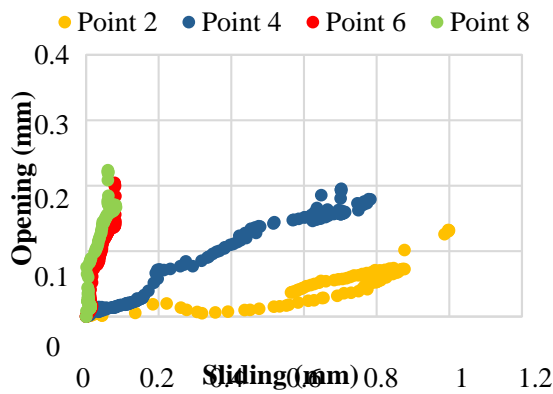
Figure 7: Selected points at the tips of ribs and between ribs for concrete and cement paste



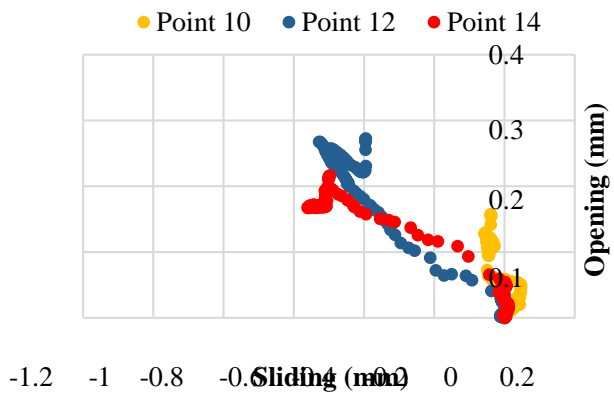
(a) Points at tips of ribs to the left of central line



(b) Points at tips of ribs to the right of central line

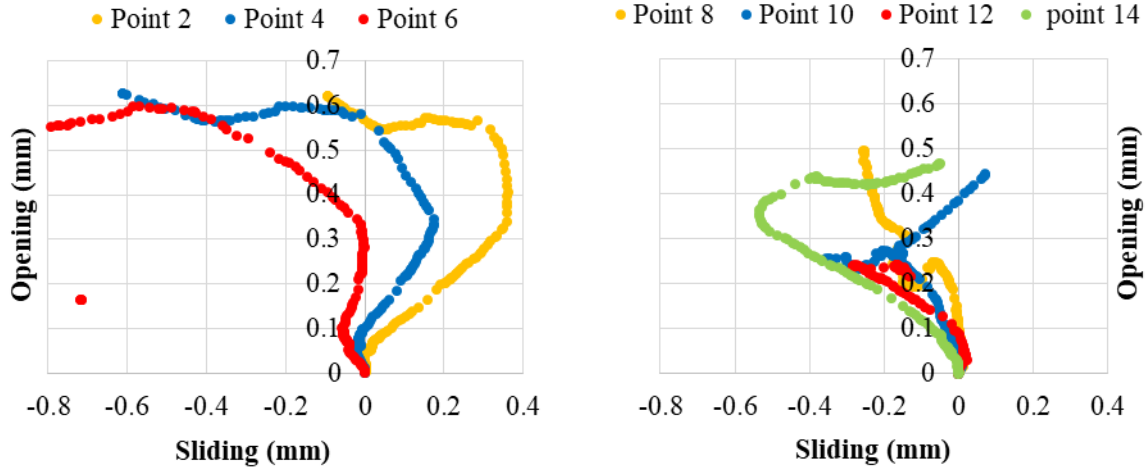


(c) Points between ribs to the left of central line



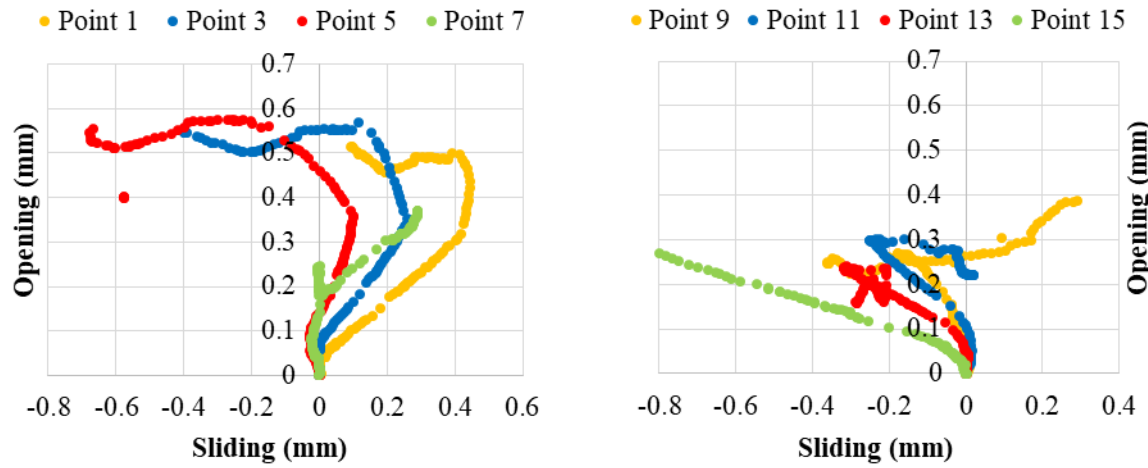
(d) Points between ribs to the right of central line

Figure 8: Opening-sliding relationships in concrete



(a) Points at tips of ribs to the left of central line

(b) Points at tips of ribs to the right of central line



(c) Points between ribs to the left of central line

(d) Points between ribs to the right of central line

Figure 9: Opening-sliding relationships in cement paste

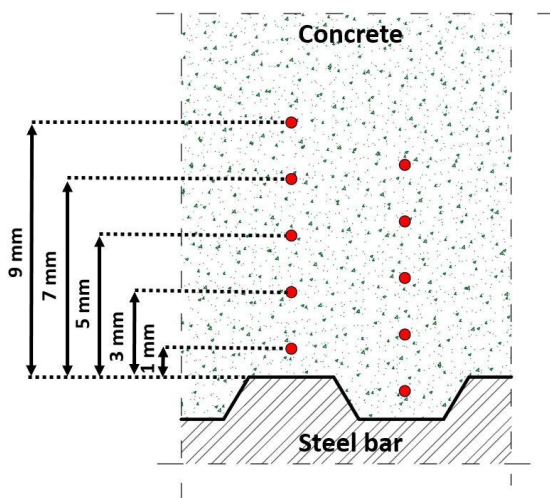


Figure 10: Lay-out for two points with different positions (1-3-5-7-9 mm).

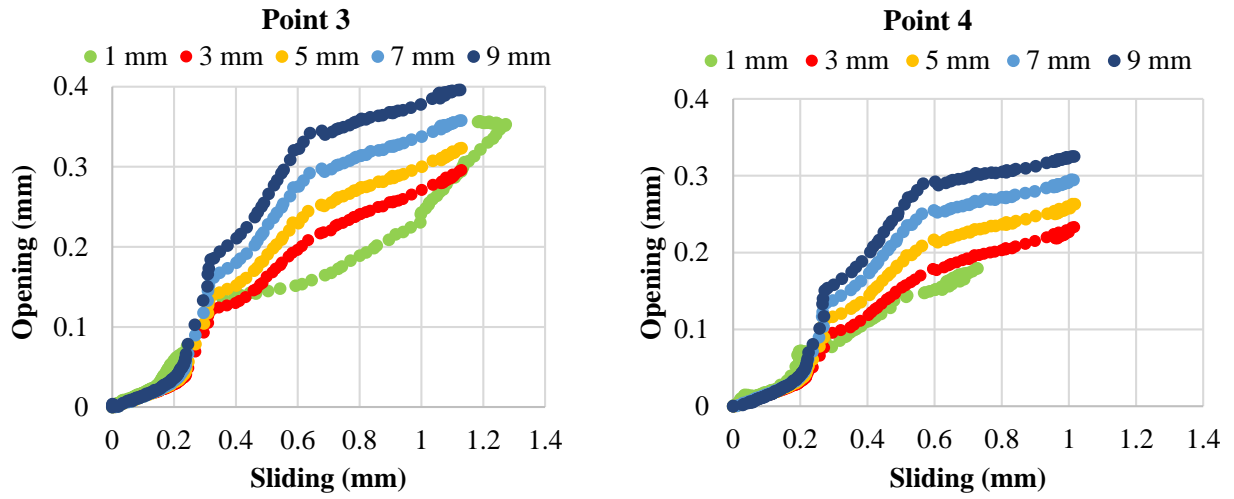


Figure 11: Opening-sliding relationship in concrete for two points at different positions (1-3-5-7-9 mm).

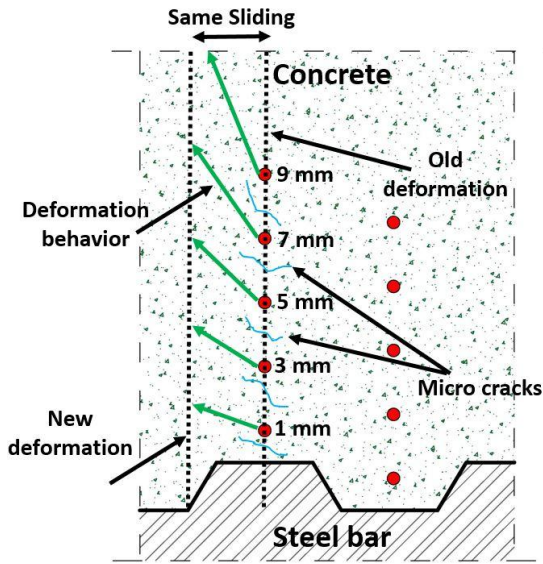


Figure 12: Schematic of opening-sliding behavior in concrete with going vertically from the rebar.